Published in final edited form as:

Circulation. 2015 May 19; 131(20): 1783–1795. doi:10.1161/CIRCULATIONAHA.114.012377.

Segmental Aortic Stiffening Contributes to Experimental Abdominal Aortic Aneurysm Development

Uwe Raaz, MD[1,2,3], **Alexander M. Zöllner, MS**[4,2], **Isabel N. Schellinger**[1,3], **Ryuji Toh, MD, PhD**[1], **Futoshi Nakagami, MD, PhD**[1,2], **Moritz Brandt, MD**[2], **Fabian C. Emrich, MD**[5,2], **Yosuke Kayama, MD, PhD**[1,2,3], **Suzanne Eken, MD**[6], **Matti Adam, MD**[1,2,3], **Lars Maegdefessel, MD, PhD**[6], **Thomas Hertel, MD**[7], **Alicia Deng**[1,3], **Ann Jagger, PhD**[1,3], **Michael Buerke, MD**[8], **Ronald L. Dalman, MD**[9,2], **Joshua M. Spin, MD, PhD**[1,2,3], **Ellen Kuhl, PhD**[4,10,5], and **Philip S. Tsao, PhD**[1,2,3]

[1]Division of Cardiovascular Medicine, Stanford University School of Medicine, Stanford, CA

[2]Cardiovascular Institute, Stanford University School of Medicine, Stanford, CA

[3]VA Palo Alto Health Care System, Palo Alto, CA

[4]Department of Mechanical Engineering, Stanford University School of Medicine, Stanford, CA

[5]Department of Cardiothoracic Surgery, Stanford University School of Medicine, Stanford, CA

[6]Department of Medicine, Karolinska Institute, Stockholm, Sweden

[7]Center for Vascular Medicine, Zwickau, Germany

[8]Division of Cardiovascular Medicine and Intensive Care Medicine, Saint Mary's Hospital, Siegen, Germany

[9]Division of Vascular Surgery, Stanford University School of Medicine, Stanford, CA

[10]Department of Bioengineering, Stanford, CA

Abstract

Background—Stiffening of the aortic wall is a phenomenon consistently observed in age and in abdominal aortic aneurysm (AAA). However, its role in AAA pathophysiology is largely undefined.

Methods and Results—Using an established murine elastase-induced AAA model, we demonstrate that segmental aortic stiffening (SAS) precedes aneurysm growth. Finite element analysis (FEA) reveals that early stiffening of the aneurysm-prone aortic segment leads to axial (longitudinal) wall stress generated by cyclic (systolic) tethering of adjacent, more compliant wall segments. Interventional stiffening of AAA-adjacent aortic segments (via external application of surgical adhesive) significantly reduces aneurysm growth. These changes correlate with reduced segmental stiffness of the AAA-prone aorta (due to equalized stiffness in adjacent segments), reduced axial wall stress, decreased production of reactive oxygen species (ROS), attenuated

Correspondence: Philip S. Tsao, PhD, VA Palo Alto Health Care System, 3801 Miranda Avenue; Building 101 #A2-141, Palo Alto, CA 94304, Phone: 650-493-5000 x62991, Fax: 650-852-3203, ptsao@stanford.edu.

Disclosures: None.

elastin breakdown, and decreased expression of inflammatory cytokines and macrophage infiltration, as well as attenuated apoptosis within the aortic wall. Cyclic pressurization of segmentally stiffened aortic segments *ex vivo* increases the expression of genes related to inflammation and extracellular matrix (ECM) remodeling. Finally, human ultrasound studies reveal that aging, a significant AAA risk factor, is accompanied by segmental infrarenal aortic stiffening.

Conclusions—The present study introduces the novel concept of segmental aortic stiffening (SAS) as an early pathomechanism generating aortic wall stress and triggering aneurysmal growth, thereby delineating potential underlying molecular mechanisms and therapeutic targets. In addition, monitoring SAS may aid the identification of patients at risk for AAA.

Keywords

aorta; aneurysm; aortic stiffness; wall stress; remodeling

Introduction

Abdominal aortic aneurysm (AAA) carries a high mortality in case of rupture[1]. Current therapies are limited to open surgical or interventional stent-based exclusion of the aneurysmal sac from the circulation in order to prevent rupture. However, these treatment options are generally reserved for larger aneurysms (typically AAA diameter>5.5 cm), and there is no effective therapy targeting the evolution of small aneurysms. This lack of treatment options partly derives from an insufficient understanding of early AAA pathogenesis.

Recent evidence suggests that AAA formation is not simply due to aortic wall degeneration, resulting in passive lumen dilation, but to active, dynamic remodeling. The latter involves transmural inflammation, extracellular matrix (ECM) alterations including elastin fragmentation and (compensatory) collagen deposition, vascular smooth muscle cell (VSMC) apoptosis, and oxidative stress[1–4].

From a patho-mechanistic point of view it is essential not only to characterize the particular cellular and molecular alterations involved in AAA formation, but also to identify early triggers of remodeling. In that respect, mechanical wall stress is an intriguing candidate. Biomechanical stress (i.e., shear stress, circumferential or axial wall stress) may drive adaptive arterial remodeling in response to altered hemodynamics, but also may induce inflammation and ECM remodeling, as well as VSMC apoptosis in vascular disease[4,5]. AAA growth is accompanied by increasing wall stress[6,7]. While wall stress due to the vessel's expanding geometry significantly contributes to eventual rupture of the "mature" AAA, it might appear that wall stress would be unrelated to the pathophysiology in early, pre-aneurysmal stages, when aortic size has not yet overtly changed. However, enhanced wall stress may still occur due to early aortic biomechanical alterations (i.e., aortic stiffening).

AAA formation is associated with a substantially increased wall stiffness[8,9]. Additionally, pronounced stiffening of the abdominal aorta occurs with aging, a major risk factor for

AAA[10]. We hypothesize that the existence of a stiff aortic segment adjacent to a more compliant aorta (i.e., segmental aortic stiffness, SAS) generates axial wall stress due to non-uniform systolic wall deformations, thereby modulating early aneurysm pathobiology (Figure 1).

Materials and Methods

Details are described in the Supplemental Material.

Porcine pancreatic elastase (PPE) infusion model

The PPE infusion model to induce AAA in 10-week-old male C57BL/6J mice was performed as previously described[11]. In brief: after placing temporary ligatures around the proximal and distal aorta, an aortotomy was created at the bifurcation and an insertion catheter was used to perfuse the aorta for 5 minutes with saline containing porcine pancreatic elastase (1.5U/mL; Sigma Aldrich).

Glue treatment of the PPE-adjacent aortic segments

In order to locally enhance aortic mechanical stiffness, a surgical adhesive (BioGlue, CryoLife, Atlanta) was applied to the segments adjacent to the PPE-treated aorta directly after completion of the PPE-treatment. Complete polymerization of the two-component glue (albumin/glutaraldehyde) occurred within seconds. Care was taken to avoid the PPE-treated segment (Supplemental Figure S1). For sham-treatment groups only one component of BioGlue was applied.

Mouse ultrasound studies

Systolic diameter (D_s) and diastolic diameter (D_d) were quantified in the PPE-treated segment as well as in the adjacent untreated segments using M-Mode ultrasound. Circumferential cyclic strain ε was calculated as $\varepsilon = (D_s - D_d)/D_d \times 100\%$. Segmental aortic stiffness (SAS) was defined as a relative index to quantify the stiffness of the PPE-treated segment in relation to the adjacent aorta, calculated as $SAS = \varepsilon_{\text{adjacent aorta}}\ \varepsilon_{\text{PPEsegment}}$. The strain values for adjacent aorta ($\varepsilon_{\text{adjacent aorta}}$) represent an average strain calculated from the adjacent segments proximal and distal to the PPE-treated segment. For shear stress calculations, blood flow was assessed as previously described[12].

Human ultrasound studies

19 male volunteers of different ages (youngest age: 36, oldest age: 71, mean age: 51.9 years) were included in the study. Exclusion criteria were cardiovascular diseases (in particular AAA), diabetes and history of smoking. M-mode images tracking the anterior and posterior aortic wall motion were recorded at predefined locations (suprarenal, mid-infrarenal and proximal to the aortic bifurcation).

Systolic diameter (D_s) and diastolic diameter (D_d) were quantified in the suprarenal, mid-infrarenal and bifurcational segment of the abdominal aorta to calculate cyclic strain and SAS.

Finite element analysis (FEA)

Finite element analyses of the mouse aorta were performed using the commercial finite element software package ABAQUS. The artery was modeled as a 2.0 mm long axisymmetric tube with outer diameter D_a=0.9 mm and arterial wall thickness t=0.075 mm. The intima, media, and adventitia were summarized in a single homogeneous layer modeled using an isotropic Neo-Hookean strain energy function with a shear modulus of 300 kPa. Stiffness of the stiff segment (l=1.0 mm) was modified as indicated.

RNA quantification

Total aortic RNA was isolated and processed for qRT-PCR using standard protocols and methods.

Laser capture microdissection (LCM)

LCM was performed as previously described[13]. F4/80-stained macrophages were micro-dissected from frozen aortic cross sections (7 μm) using a PALM MicroBeam System (Zeiss). RNA was subsequently processed for qRT-PCR using the Single Cell-to-CT Kit (Ambion).

Histology, immunofluorescence, in situ DHE staining and in situ hybridiziation

Standardized protocols were used, with details available in the Supplementary Material.

Ex vivo aortic mechanical stimulation

Abdominal aortae were explanted, cannulated and mounted in the heated vessel chamber of a pressure arteriograph system (Model 110P, Danish Myotechnology, Copenhagen, Denmark) and stretched to *in vivo* length. The aorta was then subjected to an automated pressure protocol, cyclically alternating between 80 mmHg and 120 mmHg with a frequency of 4/min for one hour. To stiffen/restrain either the complete aorta or just the central segment (to simulate segmental stiffening), a silicone cuff (SILASTIC Laboratory Tubing, inner diameter: 0.51mm; Dow Corning) was placed around the aorta (Supplemental Figure S1). After conclusion of the experiment the aorta was removed from the cannulas and processed for RNA isolation.

Statistics

Data are presented as mean ± SEM. For comparison of 2 groups Mann-Whitney test was performed; multiple groups (≥3 groups) comparison was accomplished by Kruskal-Wallis test with Dunn's post test. Ultrasound data comparing 2 groups/treatments over time were analyzed by permutation *F*-test based on 2-way repeated measures ANOVA. For each treatment assignment, we performed a repeated measures ANOVA and derived a null distribution of the p-value for treatment effect. The p-value from the permutation test was then established as the percentage of the null p-values less than the p-value from the real data. To compare ultrasound parameters within one treatment group over time Friedman's test was used. For correlation analysis of animal ultrasound data Spearman correlation was used. For correlation analyses of human ultrasound data, Pearson correlation was used after

passing D'Agostino-Pearson omnibus normality test. A value of $p \leq 0.05$ (two-sided) was considered statistically significant.

Study approval

All animal protocols were approved by the Administrative Panel on Laboratory Animal Care at Stanford University (http://labanimals.stanford.edu/) and followed the National Institutes of Health and USDA Guide lines for Care and Use of Animals in Research.

Results

Aortic stiffening precedes aneurysmal dilation in experimental AAA

We investigated the temporal relationship between aortic biomechanical alterations and aneurysmal dilation in the porcine pancreatic elastase (PPE)-infusion model of murine AAA. Circumferential cyclic aortic strain (as a measure of vascular stiffness) and aortic diameter were monitored over time in the PPE-treated segment and saline-perfused controls via M-Mode ultrasound (Figures 2A,B).

While native abdominal aortae exhibited a baseline cyclic strain of about 12%, PPE-infusion rapidly induced a substantial strain reduction of more than 50% in the treated segment at d1 followed by further declines until d14, after which it remained stable until d28. In contrast, saline infusion only resulted in a minor strain reduction in the corresponding segment (Figure 2A).

The aortic diameter, however, displayed insignificant enlargement up to d7 post-PPE and post-saline. The PPE-treated segment then dilated markedly between d7 and d14. Afterwards the aortic diameter remained relatively stable up to d28 (Figure 2B).

Investigating possible mechanisms for the rapid stiffening of the PPE-treated segments we found remarkable elastin fragmentation, while pro-fibrotic responses were only moderate (Figure 2F).

Segmental aortic stiffening generates axial wall stress in the AAA-prone segment

Having identified rapid early mechanical stiffening of the aneurysm-prone segment (i.e. reduced cyclic strain), we sought to investigate its role in aneurysm development. We hypothesized that segmental aortic stiffening (SAS; defined as enhanced stiffness of the aneurysm-prone segment relative to the adjacent aorta) would generate adverse wall stress during cyclic deformation of the aortic wall, eventually resulting in AAA formation. We therefore performed *in silico* wall stress analysis employing a finite element model.

Using a simplified approach, the infrarenal mouse aorta was modeled as a cylindrical tube. To examine the effects of segmental stiffening we simulated a pressure of 130 mmHg (approximating systolic blood pressure) and introduced a segment of increasing stiffness (SS) adjacent to a non-stiff segment (AS). We found that increasing segmental stiffness progressively induced axial stress in the stiff segment extending from the segmental interface (Figure 3A).

As hypertension represents a risk factor for AAA, we explored the impact of high blood pressure levels on axial wall stress by pressurizing our FEA model with a fixed stiffness of the stiff segment up to 180 mmHg. This simulation revealed that high blood pressure augmented segmental stiffness-based wall stresses (Figure 3B).

Taken together these data suggest that segmental aortic stiffness generates substantial axial wall stresses that also are susceptible to a hypertensive environment.

Segmental aortic stiffness correlates with experimental aneurysm progression

To further investigate the significance of segmental aortic stiffening (SAS) as an inducer of aneurysm growth we performed temporal analysis of SAS *in vivo* and correlated it to aneurysm growth in the PPE model. We found a continuous increase in SAS after aneurysm-induction, peaking at d7, which was due to increasing stiffness of the PPE-treated segment (5-fold higher than adjacent aorta; Figures 2C,D). Of note, the SAS peak coincided with the onset of aneurysm expansion. Moreover, the magnitude of SAS at d7 correlated with subsequent aortic enlargement between d7 and d14 (Figure 2E).

After d7 SAS declined as a result of progressive stiffening of the adjacent aortic segments (Figures 2C,D), which was accompanied by decelerating aortic diameter enlargement (Figure 2B). Saline-infused controls did not exhibit significantly enhanced SAS at any point during the entire observation period (Figure 2C).

Pro-fibrotic mechanisms accompany stiffening of AAA-adjacent segments, thereby reducing segmental aortic stiffness

Having detected decreased SAS at d14 due to stiffening in the AAA-adjacent aorta, we investigated the underlying molecular mechanisms.

Medial collagen deposition – a known determinant of arterial stiffness – was remarkably enhanced in AAA-adjacent segments at d14 after aneurysm induction (compared to d7; Figure 4D). Expression of the collagen genes *Col1a1* and *Col3a1* was increased in the adjacent segments compared to the AAA segment itself at d7 (Figure 4A), preceding the histological alterations. In line with this observation, miR-29b – previously shown to be an epigenetic negative regulator of collagen expression in AAA – was similarly downregulated at d7 (Figure 4B). More specifically, *in situ* hybridization (ISH) indicated marked miR-29b downregulation within the aortic media (Figure 4C).

In contrast to the marked pro-fibrotic changes elastin architecture appeared unaffected in the AAA-adjacent aorta (Figure 4D).

Interventional reduction of segmental stiffness reduces wall stress and aneurysm progression

To investigate the potential causative role of segmental aortic stiffening as a mechanism driving AAA development we focally stiffened the adjacent aorta next to the PPE-treated segment by peri-aortic application of BioGlue, a surgical adhesive with a relatively high material stiffness (Supplemental Figure S2). Glue application induced rapid and sustained stiffening of the adjacent aortic segments (Figure 5A), resulting in near-equalization of

stiffness between the PPE-treated segment and the glue-treated adjacent segments. This was reflected in a significant reduction of SAS compared to sham-glue treated controls (Figure 5B).

To exclude the possibility that aortic constriction due to segmental glue treatment might lead to alterations of the downstream aortic flow and fluid shear stress, thereby affecting aneurysm formation, we monitored the aortic diameter of the glue-treated segment as well as the downstream flow profile. We detected neither luminal narrowing (data not shown) nor elevated flow shear stress levels (Supplemental Figure S3). Glue-treatment of the adjacent aorta did not cause perturbations of its elastin architecture nor an enhanced fibrotic response (Supplemental Figure S4), suggesting that direct mechanical interaction with the aortic wall caused the stiffening effect.

Further, our finite element model demonstrated that stiffness equalization between all segments (i.e., reduction of SAS) resulted in decreased and homogenized axial stress (Figure 3C).

Finally, comparing aortic diameter between glue-treated and sham-glue-treated animals we found that PPE-induced aortic expansion was significantly reduced when adjacent segments were immobilized by glue application. The expected rapid diameter increase between d7 and d14 was suppressed (Figure 5C).

To further test the efficiency of delayed glue treatment on aneurysm progression we performed additional experiments with glue intervention at d7 post PPE, when there already is a small dilation combined with a high segmental stiffness (Figures 5D,E). As a result we found that delayed glue-stiffening of the AAA-adjacent aorta also significantly reduces SAS and thereby represses the consecutive aneurysmal diameter progression compared to sham-glue treated animals (Figures 5D,E).

Reduction of segmental stiffness modulates critical features of AAA pathobiology

Since AAA formation is accompanied by extensive extracellular matrix (ECM) remodeling, we performed histologic analyses of the aneurysm wall, focusing on elastin and collagen architecture. Extensive destruction of elastin fibers – a hallmark of aneurysm pathology – was present in sham-glue-treated mice on d14 after PPE infusion (Figure 5F). Further, Picrosirius Red staining revealed disturbed wall architecture with general wall thickening, loss of layered structure, and diffuse collagen enrichment (Figure 5G). In contrast, elastin structure and wall layering was better preserved in the glue-treated group while collagen accumulation appeared less prominent (Figures 5F,G).

AAA pathology includes enhanced reactive oxygen species (ROS) generation, vascular inflammation, vascular smooth muscle cell (VSMC) apoptosis and enhanced MMP activity. To assess the impact of SAS-modulations on these endpoints we analyzed the PPE-treated aorta at d7, which marks the peak of segmental stiffening but precedes the prominent diameter increase between d7 and d14.

We performed *in situ* dihydroethidium (DHE) fluorescence to monitor ROS generation. PPE-treated segments exhibited enhanced nuclear fluorescence compared to native controls while glue treatment resulted in a significant decrease in ROS production (Figures 6A,B).

Inflammation was quantified by aortic macrophage infiltration and cytokine analysis. Extensive macrophage infiltration of the aortic wall was present 7 days after aneurysm induction as assessed by immunofluorescence (Figures 6C–E), accompanied by enhanced aortic gene expression of *Il6, Ccl2* and *Il1b* (Figure 6G). Immunofluorescence additionally revealed macrophage co-localization with each of these cytokines (Supplemental Figure S5). Glue treatment reduced macrophage infiltration as well as cytokine expression (Figures 6C,D,E).

To further delineate the role of macrophages in vascular cytokine production we analyzed gene expression profiles of macrophages directly isolated from the PPE-aneurysm sections via laser capture microdissection (LCM). To this end we micro-dissected macrophages (positive F4/80 staining) from the aortic wall and confirmed macrophage transcript enrichment by enhanced *Emr1* expression (encoding for F4/80 protein) compared to randomly captured F4/80-negative cells (Supplemental Figure S6). Macrophages isolated from sham-glue treatment exhibited significantly higher expression of *Il1b, Il6* and *Ccl2* compared to those from glue-stiffened samples (Figure 6H).

Assessing apoptosis, we detected enhanced capase-3 activity in the intimal and medial layer of PPE-treated aortic wall, which was reduced in the glue-treated group (Figure 6F). MMP2 and MMP9 are essential for matrix macromolecule degradation in AAA. In accordance with the substantial elastin breakdown found in PPE-treated segments, both *Mmp2* and *Mmp9* were significantly upregulated. Glue-stabilization of the adjacent aortic segments – which prevented extensive elastin breakdown and collagen remodeling – minimized Mmp expression (Figure 6I). Additionally, this intervention reduced enhancement of *Col1a1* and *Col3a1* expression after aneurysm induction (Figure 6J).

Ex vivo segmental aortic stiffening induces upregulation of AAA-related genes

We examined the mechanism of SAS as a driver of AAA pathogenesis by validating our *in vivo* findings *ex vivo*. We explanted murine abdominal aortic segments and mounted them onto a pressure myograph system. Aortae were then subjected to physiologic pressure levels, cyclically alternating between 80mmHg and 120mmHg. To simulate aortic stiffening, the “systolic” expansion of either the entire aortic segment (complete stiffening) or just the central aortic segment (segmental stiffening) was restrained by an externally applied silicone cuff (Figure 7A, Supplemental Figure S6). After one hour of cyclic pressurization, aortic gene expression was analyzed.

Cuffing the entire aortic segment had minimal-to-no effect on the expression of inflammatory cytokines *Il6* and *Ccl2*. Segmental stiffening, in contrast, induced upregulation of these genes (Figure 7B). Likewise, the expression of metalloproteinases (*Mmp2, Mmp9*) as well as collagen genes (*Col1a1, Col3a1*) – quantified as indicators of active matrix remodeling – was significantly enhanced only in response to segmental stiffening (Figures 7C,D).

The aging human abdominal aorta exhibits segmental stiffening

In order to test whether SAS occurs naturally in the human aorta, we assessed the aortic stiffness in three distinct locations (suprarenal, mid-infrarenal, bifurcational) along the abdominal aortas of 19 male patients ranging in age from 36 to 71 years without evident AAA.

A significant negative correlation was observed between age and aortic cyclic strain in the suprarenal and mid-infrarenal as well as in the aortic bifurcation segments, suggesting generally enhanced stiffness in the aging abdominal aorta (Figures 8A,B,C).

We also detected important differences between the distinct aortic locations. While both the mid-infrarenal aorta and the bifurcation exhibited age-related strain reduction, the slope of strain reduction was significantly steeper in the bifurcation segment, altering the (relative) SAS between two regions. In younger patients the stiffness between both segments was similar (SAS~1), but doubled (SAS~2) by age 60 (Figure 8D). These results indicate that in addition to overall stiffening of the abdominal aorta with age, the human abdominal aorta exhibits age-related segmental stiffening.

Discussion

AAA formation is accompanied by increased stiffness of the aneurysmal vessel segment compared to the normal aorta[9,14]. Aneurysmal stiffening occurs due to profound changes in ECM organization including elastin fragmentation and enhanced adventitial collagen deposition and turnover[14]. The current study was designed to investigate aortic stiffening as a potential factor driving early AAA pathogenesis.

To explore the temporal relationship between aortic stiffening and AAA growth we employed the widely-used PPE animal model. As human AAA typically occurs in the aged aorta, which exhibits progressive elastin degeneration and stiffening[10,15], we deliberately chose the PPE model as a non-dissection type preclinical model of AAA because it not only phenotypically resembles many aspects of the human disease but is also initiated by mild destruction of the elastin architecture (although this is achieved enzymatically by PPE perfusion in contrast to fatigue-related elastin fracture in the human situation). Moreover, our previous studies indicated that this model in particular appears sensitive to extracellular matrix/stiffness related interventions[16].

Our data confirm that aortic stiffening precedes aneurysmal dilation[17]. The rapid stiffening which occurred within one day after treatment seems to be due to early PPE-induced elastin damage (Figure 2F). However, PPE is biologically active for no more than 24h after perfusion[18]. Therefore, later structural alterations of the aorta, including the pervasive elastin fragmentation observed after 14 days (Figure 5F), appear to be PPE-independent.

Although the observed early and sustained stiffening of the aneurysm-prone aorta may seem counterintuitive, this finding supports aneurysm growth as an active process, as opposed to simple passive dilation. Moreover, segmental stiffening of the abdominal aorta may qualify as a mechanism generating wall stress.

Mechanical stress is a potent inducer of physiologic arterial remodeling. High flow-induced shear stress, elevated circumferential stress, and increased axial stress result in increased vessel diameter, wall thickening, and arterial lengthening, respectively, to achieve stress normalization[5]. From a pathogenic point of view, mechanical forces induce a multitude of adverse events contributing to vascular disease, including ROS generation, apoptosis, and inflammation[4,19–21].

To test the hypothesis that SAS generates wall stress that precedes and triggers early AAA growth, we carried out *in silico* stress-analysis employing a FEA model. Inclusion of a stiff segment in a more compliant aorta generates axial stress under systolic pressurization. Axial stress increases with enhanced stiffness-gradients between stiff and non-stiff segments (Figure 3A). Hypertension, a known AAA-associated risk factor, further increases axial stress in the setting of SAS (Figure 3B). Of note, this simplified model only takes into account static wall stresses, neglecting dynamic effects that may occur due to cyclic systolic-diastolic wall deformations.

In our animal model the peak of SAS at d7 coincided with the onset of accelerated aneurysmal enlargement. Delayed AAA formation until 7 days after PPE-treatment is consistent with the initial characterization of this model[6]. The relationship between increasing SAS and subsequent aneurysmal dilation was further strengthened by a positive correlation between the extent of SAS at d7, and aortic diameter enlargement between d7 and d14.

To clarify the pathophysiologic significance of SAS for AAA-growth we selectively applied rapid-hardening biologic glue to the aortic segments adjacent to the PPE-injury site, achieving dramatic stiffening of the adjacent aorta, detectable within one day after intervention. Subsequently, the relative segmental stiffness of the PPE-treated aorta compared to its adjacent segments (i.e, SAS) was instantly and permanently reduced. A major finding of this study is that the (glue-induced) reduction in SAS translated into significantly reduced AAA growth. In a more therapeutic context we additionally found delayed glue application (day7 post PPE injury) to reduce subsequent AAA progression.

To elucidate the mechanisms of this process we analyzed factors that contribute to AAA, and that are moreover known to be mechanosensitive: ROS generation, inflammation, ECM-remodeling and apoptosis. ROS levels are locally increased in human AAA compared to the adjacent non-aneurysmal aorta[22]. ROS may be generated in response to mechanical stress in endothelial cells (ECs) as well as in vascular smooth muscle cells (VSMCs), whereby mechanically activated NADPH oxidases (NOX) and the mitochondrial electron transport chain seem to be significant sources[23,24]. Mechanically generated ROS may subsequently trigger a variety of cellular responses such as VSMC apoptosis[25] and vascular inflammation[4]. ROS-scavengers and NADPH-oxidase inhibition have reduced oxidative stress and aortic macrophage infiltration, and ultimately ameliorated aneurysm growth or decreased aneurysm rupture incidence in various murine AAA models[26–28]. We found decreased ROS generation following glue-mediated reduction of SAS and axial stress.

AAA-formation is characterized by inflammatory remodeling of the aortic wall, and vascular inflammatory reactions are sensitive to mechanical stress-induced signaling. For example, mechanical stress induced pro-inflammatory mechanisms involve enhanced cytokine production via Ras/Rac1-p38-MAPK-NF-κB (leading to enhanced IL-6 expression in VSMC)[20], as well as enhanced NF-κB-dependent expression of vascular chemokines and adhesion molecules that facilitate monocyte adhesion to the vascular wall[21]. Interestingly, inflammatory cells such as monocytes/macrophages become mechanosensitive once attached to the vascular ECM[29]. We show that interventional stiffening of the adjacent aorta decreases macrophage infiltration in the aneurysm-prone (PPE-treated) segment and reduces the aortic and macrophage-specific expression of various inflammatory cytokines that are known to be critical for AAA pathogenesis, including Il1b, Il6 and Ccl2[30–32]

ECM remodeling, with enzymatic breakdown of matrix macromolecules mediated by the metalloproteinases MMP-2 and MMP-9, is another hallmark of AAA. MMP expression is increased in human AAA[33–35], and knockout of MMP-2 and MMP-9 abolishes experimental AAA formation[18,36]. MMP-2 and MMP-9 are also responsive to mechanical stress due to cyclic stretch and enhanced flow[24,37]. More importantly, axial stress induces tissue remodeling and Mmp-2 activation in a model of longitudinal carotid growth[38]. As expected, *Mmp2* and *Mmp9* were significantly upregulated in PPE-treated aorta (Figure 6I). Reducing SAS, and thereby cyclic axial stress, with glue-stiffening reduced expression of both MMPs.

VSMC apoptosis is another critical feature of human and experimental AAA[39,40], and susceptible to enhanced mechanical (axial) stress[38]. Signaling mechanisms of mechanical stress-induced VSMC apoptosis include a variety of molecules, such as the endothelin B receptor, integrinβ1-rac-p38-p53 signaling or Bcl-2-associated death factor (BAD)[19]. We identified enhanced medial layer apoptosis in PPE-treated segments, which was decreased by glue-mediated axial stress reduction.

We further investigated the impact of SAS on inflammation and matrix remodeling *ex vivo*. Segmental stiffening (induced with an external cuff around the cyclically-pressurized aorta) resulted in significant upregulation of *Mmp2* and *Mmp9, Col1a1 and Col3a1*, as well as *Il6* and *Ccl2*. In contrast to the *in vivo* situation, where enhanced bi-axial stiffness results from alterations of the inherent material properties of the vessel wall, our *ex vivo* model only simulated circumferential stiffening by external cuffing. Due to technical limitations, our systolic and diastolic pressure levels alternated with a frequency of 3/min (normal C57BL/6 heart rate:~450/min[41]). Nevertheless, the data indicate that cyclic axial mechanical stress may directly control genes governing inflammation and matrix remodeling.

We observed stiffening of the aneurysm-adjacent aorta at d14 after PPE-induction, with subsequent reduction of aneurysm growth rate. This might represent an endogenous compensatory mechanism to reduce SAS and contain AAA progression. The stiffening process was paralleled by an enhanced fibrotic response in the AAA-adjacent segments' media, including upregulated collagen expression. A previous study showed that microRNA(miR)-29b is a repressor of collagen expression in AAA[16]. We identified analogous miR-29b downregulation in the (VSMC-dominated) media of the AAA-adjacent aortic segments, consistent with miR-29b-modulated VSMC collagen production and medial

fibrosis. We previously demonstrated that forced miR-29b downregulation (via systemic "anti-miR" administration) is a pro-fibrotic intervention reducing AAA growth[16]. This reduction, in light of the present study, may be partially due to accelerated miR-29b-dependent stiffening of the AAA-adjacent aorta.

Local aortic PPE infusion is a widely used preclinical AAA model that exhibits many features seen in human AAA, including early disturbance of elastin integrity. However, due to the artificial, invasive nature of the model, including enzymatic injury of the vessel, segmental stiffness might be model-specific, and not a feature of human AAA. We therefore studied whether the human abdominal aorta exhibits segmental stiffness that – according to our hypothesis – would be a contributing factor for AAA formation. Performing ultrasound-based strain analyses in three distinct locations along the abdominal aorta (suprarenal, mid-infrarenal, bifurcation) we detected age-dependent reduction of strain (increased stiffness), corresponding to previous observations[42]. As a novel finding, we detected relatively more pronounced stiffening of the aortic bifurcation segment with age (Figure 8C), translating into increasing SAS of the aortic bifurcation over time (Figure 8D). This distal part of the aorta has relatively low elastin content as compared to the more proximal segments[43], a feature that might become functionally relevant with age-dependent loss of elastin[15]. These data confirm and refine previous observations of enhanced age-dependent stiffening of the abdominal aorta[10] and might partly explain the significant influence of age on AAA risk.

Of note, the segmental stiffness we observed in the human abdominal aorta (SAS~2) was significantly smaller than the peak segmental stiffness in the PPE-treated aorta (SAS~5). The study patients presumably exhibited "physiologic" stiffness segmentation that will most likely not result in AAA formation. However, segmental stiffening may have more dramatic effects in individuals with genetic predilection for aneurysm formation.

In conclusion, the present study introduces the novel concept of segmental aortic stiffening as a pathogenetic factor contributing to AAA. We propose that degenerative stiffening of the aneurysm-prone aortic wall leads to axial stress, generated by cyclic tethering of adjacent more compliant wall segments. Axial stress then induces and augments processes necessary for AAA growth such as inflammation and vascular wall remodeling (Supplemental Figure S7). Clarification of these biomechanical signaling pathways may lead to additional therapeutic targets.

From a diagnostic point of view, AAA characterization has almost exclusively focused on the dilated segment. In light of the present findings, additional mechanical characterization of the AAA-adjacent aortic segments might provide important insights into the "stress status" of the aneurysm. This might be of particular relevance in early (even pre-aneurysmal) stages of disease, when mechanical stress is not yet predominantly driven by large geometric alterations. For instance, ultrasound-derived SAS-assessment might help to predict the susceptibility for AAA formation and future AAA growth. Therefore SAS could practically be useful to individualize risk prediction for patient populations at generally increased risk for AAA (e.g., smokers, family history) or to better determine monitoring intervals for patients with small AAA. Having a more sensitive and specific indicator for

clinical progression may improve decision-making in AAA disease, and help direct resources to those in need in an increasingly resource-constrained environment.

From a therapeutic perspective, this study suggests that mechanically stiffening the AAA-adjacent aorta might provide a “stress shield” to limit AAA remodeling and expansion. This is supported in principle by recent data suggesting reduced growth rate of suprarenal AAAs in patients having undergone endovascular repair of a concomitant infrarenal AAA (compared to control patients without infrarenal repair)[44]. Of note, protective interventional stiffening of an AAA-adjacent segment may create a distal stiffness gradient along the arterial tree that potentially triggers distal aneurysm formation. However, we did not observe any evidence of this during the 28-day time course of our model. This may indicate that in addition to stiffness gradients other predisposing co-factors (e.g., a structurally impaired vessel matrix) may be required to trigger AAA formation *de novo*. Further, we did not detect increased blood pressure levels after interventional stiffening of the abdominal aorta that could potentially point towards negative hemodynamic side effects (Supplemental Table S1). Therefore, interventional stiffening of the aortic segment next to a small aneurysm could be further tested as a novel approach to limit further AAA progression, and forestall surgical repair.

Supplementary Material

Refer to Web version on PubMed Central for supplementary material.

Acknowledgments

We would like to thank Tiffany K. Koyano, Yanli Wang, Michelle Ramseier and Brian Deng for expert technical assistance. We further thank Hui Wang, Ying Lu, Balasubramanian Narasimhan and Bradley Efron for expert statistical consulting.

Funding Sources: This work was supported by research grants from the NIH (1R01HL105299 to P.S. Tsao), the Deutsche Forschungsgemeinschaft (RA 2179/1-1 to U. Raaz), the Stanford Graduate Fellowship (William R. and Sara Hart Kimball Fellowship to A. M. Zöllner), the University of Erlangen-Nuremberg School of Medicine (to I. N. Schellinger), and the Stanford Cardiovascular Institute (to J.M. Spin).

References

1. Nordon I, Hinchliffe R, Loftus I, Thompson M. Pathophysiology and epidemiology of abdominal aortic aneurysms. Nat Rev Cardiol. 2011; 8:92–102. [PubMed: 21079638]
2. Shah P. Inflammation, metalloproteinases, and increased proteolysis: an emerging pathophysiological paradigm in aortic aneurysm. Circulation. 1997; 96:2115–7. [PubMed: 9337176]
3. Ailawadi G, Eliason JL, Upchurch GR. Current concepts in the pathogenesis of abdominal aortic aneurysm. J Vasc Surg. 2003; 38:584–588. [PubMed: 12947280]
4. Raaz U, Toh R, Maegdefessel L, Adam M, Nakagami F, Emrich F, Spin J, Tsao P. Hemodynamic regulation of reactive oxygen species: implications for vascular diseases. Antioxid Redox Signal. 2014; 20:914–28. [PubMed: 23879326]
5. Hoefer I, den Adel B, Daemen M. Biomechanical factors as triggers of vascular growth. Cardiovasc Res. 2013; 99:276–83. [PubMed: 23580605]
6. Vorp D. Biomechanics of abdominal aortic aneurysm. J Biomech. 2007; 40:1887–902. [PubMed: 17254589]
7. Humphrey J, Holzapfel G. Mechanics, mechanobiology, and modeling of human abdominal aorta and aneurysms. J Biomech. 2012; 45:805–14. [PubMed: 22189249]

8. MacSweeney S, Young G, Greenhalgh R, Powell J. Mechanical properties of the aneurysmal aorta. Br J Surg. 1992; 79:1281–4. [PubMed: 1486417]
9. Vande Geest J, Sacks M, Vorp D. The effects of aneurysm on the biaxial mechanical behavior of human abdominal aorta. J Biomech. 2006; 39:1324–34. [PubMed: 15885699]
10. Hickson S, Butlin M, Graves M, Taviani V, Avolio A, McEniery C, Wilkinson I. The relationship of age with regional aortic stiffness and diameter. JACC Cardiovasc Imaging. 2010; 3:1247–55. [PubMed: 21163453]
11. Azuma J, Asagami T, Dalman R, Tsao P. Creation of murine experimental abdominal aortic aneurysms with elastase. J Vis Exp. 2009; 29:1280. [PubMed: 19629030]
12. Hong G, Lee J, Robinson J, Raaz U, Xie L, Huang N, Cooke J, Dai H. Multifunctional in vivo vascular imaging using near-infrared II fluorescence. Nat Med. 2012; 18:1841–6. [PubMed: 23160236]
13. Sho E, Sho M, Nanjo H, Kawamura K, Masuda H, Dalman RL. Comparison of cell-type-specific vs transmural aortic gene expression in experimental aneurysms. J Vasc Surg. 2005; 41:844–52. [PubMed: 15886670]
14. He C, Roach M. The composition and mechanical properties of abdominal aortic aneurysms. J Vasc Surg. 1994; 20:6–13. [PubMed: 8028090]
15. Fritze O, Romero B, Schleicher M, Jacob M, Oh D, Starcher B, Schenke-Layland K, Bujan J, Stock U. Age-related changes in the elastic tissue of the human aorta. J Vasc Res. 2012; 49:77–86. [PubMed: 22105095]
16. Maegdefessel L, Azuma J, Toh R, Merk D, Deng A, Chin J, Raaz U, Schoelmerich A, Raiesdana A, Leeper N, McConnell M, Dalman R, Spin J, Tsao P. Inhibition of microRNA-29b reduces murine abdominal aortic aneurysm development. J Clin Invest. 2012; 122:497–506. [PubMed: 22269326]
17. Goergen C, Azuma J, Barr K, Magdefessel L, Kallop D, Gogineni A, Grewall A, Weimer R, Connolly A, Dalman R, Taylor C, Tsao P, Greve J. Influences of aortic motion and curvature on vessel expansion in murine experimental aneurysms. Arterioscler Thromb Vasc Biol. 2011; 31:270–9. [PubMed: 21071686]
18. Pyo R, Lee J, Shipley J, Curci J, Mao D, Ziporin S, Ennis T, Shapiro S, Senior R, Thompson R. Targeted gene disruption of matrix metalloproteinase-9 (gelatinase B) suppresses development of experimental abdominal aortic aneurysms. J Clin Invest. 2000; 105:1641–9. [PubMed: 10841523]
19. Qiu J, Zheng Y, Hu J, Liao D, Gregersen H, Deng X, Fan Y, Wang G. Biomechanical regulation of vascular smooth muscle cell functions: from in vitro to in vivo understanding. J R Soc Interface. 2014; 11:20130852. [PubMed: 24152813]
20. Zampetaki A, Zhang Z, Hu Y, Xu Q. Biomechanical stress induces IL-6 expression in smooth muscle cells via Ras/Rac1-p38 MAPK-NF-kappaB signaling pathways. Am J Physiol Heart Circ Physiol. 2005; 288:H2946–54. [PubMed: 15681696]
21. Riou S, Mees B, Esposito B, Merval R, Vilar J, Stengel D, Ninio E, van Haperen R, de Crom R, Tedgui A, Lehoux S. High pressure promotes monocyte adhesion to the vascular wall. Circ Res. 2007; 100:1226–33. [PubMed: 17395876]
22. Miller FJ. Oxidative Stress in Human Abdominal Aortic Aneurysms: A Potential Mediator of Aneurysmal Remodeling. Arterioscler Thromb Vasc Biol. 2002; 22:560–565. [PubMed: 11950691]
23. Matsushita H, Lee K, Tsao P. Cyclic strain induces reactive oxygen species production via an endothelial NAD(P)H oxidase. J Cell Biochem Suppl. 2001; (Suppl 36):99–106. [PubMed: 11455575]
24. Grote K, Flach I, Luchtefeld M, Akin E, Holland S, Drexler H, Schieffer B. Mechanical stretch enhances mRNA expression and proenzyme release of matrix metalloproteinase-2 (MMP-2) via NAD(P)H oxidase-derived reactive oxygen species. Circ Res. 2003; 92:e80–6. [PubMed: 12750313]
25. Li P, Dietz R, von Harsdorf R. Reactive oxygen species induce apoptosis of vascular smooth muscle cell. FEBS Lett. 1997; 404:249–52. [PubMed: 9119073]
26. Gavrila D, Li W, McCormick M, Thomas M, Daugherty A, Cassis L, Miller FJ, Oberley L, Dellsperger K, Weintraub N. Vitamin E inhibits abdominal aortic aneurysm formation in

angiotensin II-infused apolipoprotein E-deficient mice. Arterioscler Thromb Vasc Biol. 2005; 25:1671–7. [PubMed: 15933246]

27. Nakahashi T, Hoshina K, Tsao P, Sho E, Sho M, Karwowski J, Yeh C, Yang R, Topper J, Dalman R. Flow loading induces macrophage antioxidative gene expression in experimental aneurysms. Arterioscler Thromb Vasc Biol. 2002; 22:2017–22. [PubMed: 12482828]
28. Xiong W, Mactaggart J, Knispel R, Worth J, Zhu Z, Li Y, Sun Y, Baxter B, Johanning J. Inhibition of reactive oxygen species attenuates aneurysm formation in a murine model. Atherosclerosis. 2009; 202:128–34. [PubMed: 18502427]
29. Yang JH, Sakamoto H, Xu EC, Lee RT. Biomechanical regulation of human monocyte/ macrophage molecular function. Am J Pathol. 2000; 156:1797–804. [PubMed: 10793091]
30. Johnston WF, Salmon M, Su G, Lu G, Stone ML, Zhao Y, Owens GK, Upchurch GR Jr, Ailawadi G. Genetic and pharmacologic disruption of interleukin-1beta signaling inhibits experimental aortic aneurysm formation. Arterioscler Thromb Vasc Biol. 2013; 33:294–304. [PubMed: 23288154]
31. Tieu BC, Lee C, Sun H, Lejeune W, Recinos A 3rd, Ju X, Spratt H, Guo DC, Milewicz D, Tilton RG, Brasier AR. An adventitial IL-6/MCP1 amplification loop accelerates macrophage-mediated vascular inflammation leading to aortic dissection in mice. J Clin Invest. 2009; 119:3637–51. [PubMed: 19920349]
32. Moehle C, Bhamidipati C, Alexander M, Mehta G, Irvine J, Salmon M, Upchurch GJ, Kron I, Owens G, Ailawadi G. Bone marrow-derived MCP1 required for experimental aortic aneurysm formation and smooth muscle phenotypic modulation. J Thorac Cardiovasc Surg. 2011; 142:1567–74. [PubMed: 21996300]
33. Freestone T, Turner R, Coady A, Higman D, Greenhalgh R, Powell J. Inflammation and matrix metalloproteinases in the enlarging abdominal aortic aneurysm. Arterioscler Thromb Vasc Biol. 1995; 15:1145–51. [PubMed: 7627708]
34. Thompson R, Holmes D, Mertens R, Liao S, Botney M, Mecham R, Welgus H, Parks W. Production and localization of 92-kilodalton gelatinase in abdominal aortic aneurysms. An elastolytic metalloproteinase expressed by aneurysm-infiltrating macrophages. J Clin Invest. 1995; 96:318–26. [PubMed: 7615801]
35. Davis V, Persidskaia R, Baca-Regen L, Itoh Y, Nagase H, Persidsky Y, Ghorpade A, Baxter B. Matrix metalloproteinase-2 production and its binding to the matrix are increased in abdominal aortic aneurysms. Arterioscler Thromb Vasc Biol. 1998; 18:1625–33. [PubMed: 9763536]
36. Longo G, Xiong W, Greiner T, Zhao Y, Fiotti N, Baxter B. Matrix metalloproteinases 2 and 9 work in concert to produce aortic aneurysms. J Clin Invest. 2002; 110:625–32. [PubMed: 12208863]
37. Castier Y, Brandes R, Leseche G, Tedgui A, Lehoux S. p47phox-dependent NADPH oxidase regulates flow-induced vascular remodeling. Circ Res. 2005; 97:533–40. [PubMed: 16109921]
38. Jackson ZS. Wall Tissue Remodeling Regulates Longitudinal Tension in Arteries. Circ Res. 2002; 90:918–925. [PubMed: 11988494]
39. Maegdefessel L, Azuma J, Toh R, Deng A, Merk D, Raiesdana A, Leeper N, Raaz U, Schoelmerich A, McConnell M, Dalman R, Spin J, Tsao P. MicroRNA-21 Blocks Abdominal Aortic Aneurysm Development and Nicotine-Augmented Expansion. Sci Transl Med. 2012; 4:122ra22.
40. Thompson R, Liao S, Curci J. Vascular smooth muscle cell apoptosis in abdominal aortic aneurysms. Coron Artery Dis. 1997; 8:623–31. [PubMed: 9457444]
41. Hoit B, Kiatchoosakun S, Restivo J, Kirkpatrick D, Olszens K, Shao H, Pao Y, Nadeau J. Naturally occurring variation in cardiovascular traits among inbred mouse strains. Genomics. 2002; 79:679–85. [PubMed: 11991717]
42. O'Rourke M, Hashimoto J. Mechanical factors in arterial aging: a clinical perspective. J Am Coll Cardiol. 2007; 50:1–13. [PubMed: 17601538]
43. Halloran B, Davis V, McManus B, Lynch T, Baxter B. Localization of aortic disease is associated with intrinsic differences in aortic structure. J Surg Res. 1995; 59:17–22. [PubMed: 7630123]

44. Herdrich B, Murphy E, Wang G, Jackson B, Fairman R, Woo E. The fate of untreated concomitant suprarenal aortic aneurysms after endovascular aneurysm repair of infrarenal aortic aneurysms. J Vasc Surg. 2013; 58:1201–6. [PubMed: 23830316]

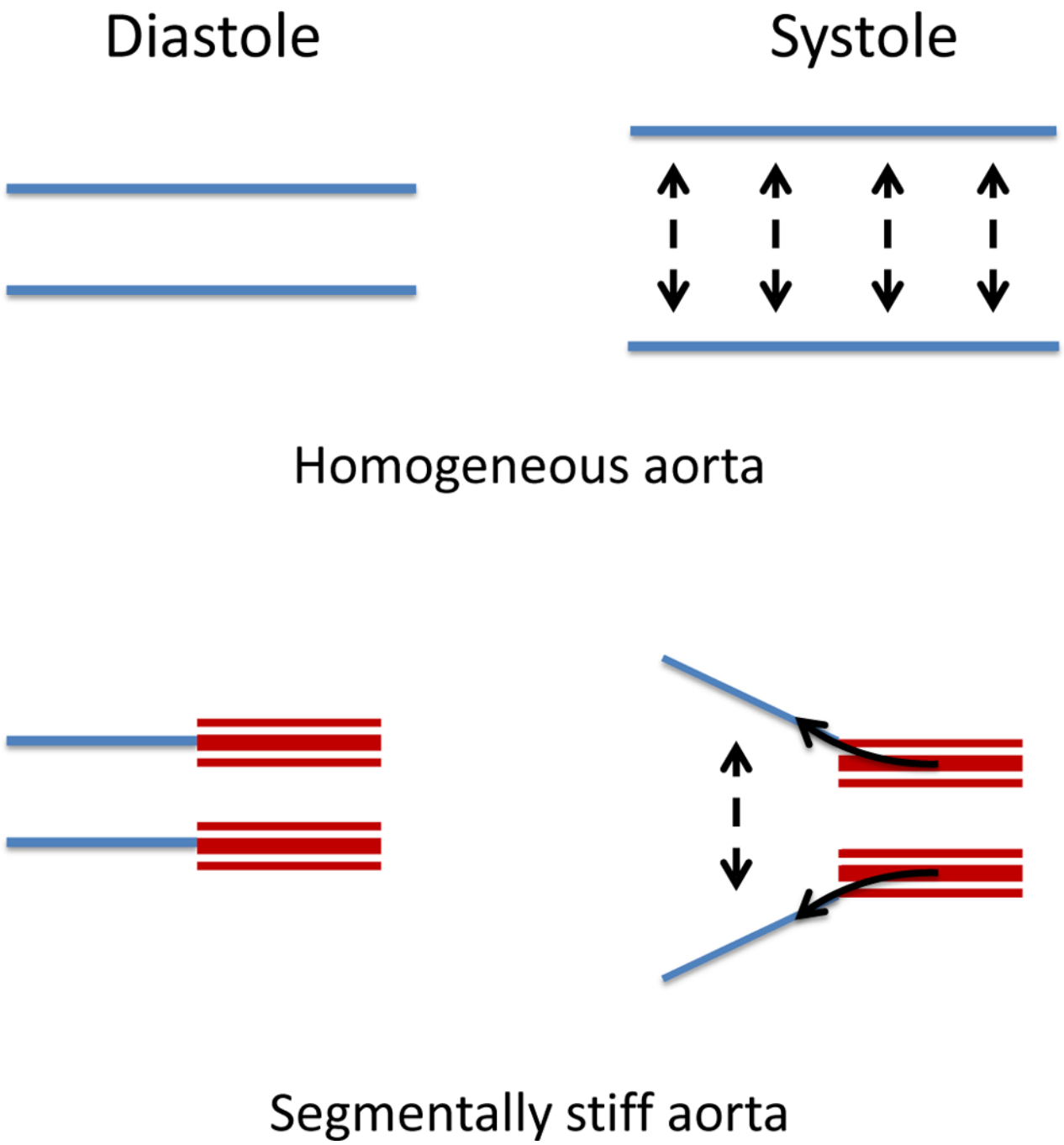

Figure 1.

Concept of Segmental Aortic Stiffness (SAS) generating axial wall stress during systolic aortic expansion. In contrast to a homogenous expandable vessel a segmentally stiff aorta (stiff segment in red) is subjected to axially tethering forces (solid arrows) during the systolic circumferential expansion of the adjacent compliant wall segments.

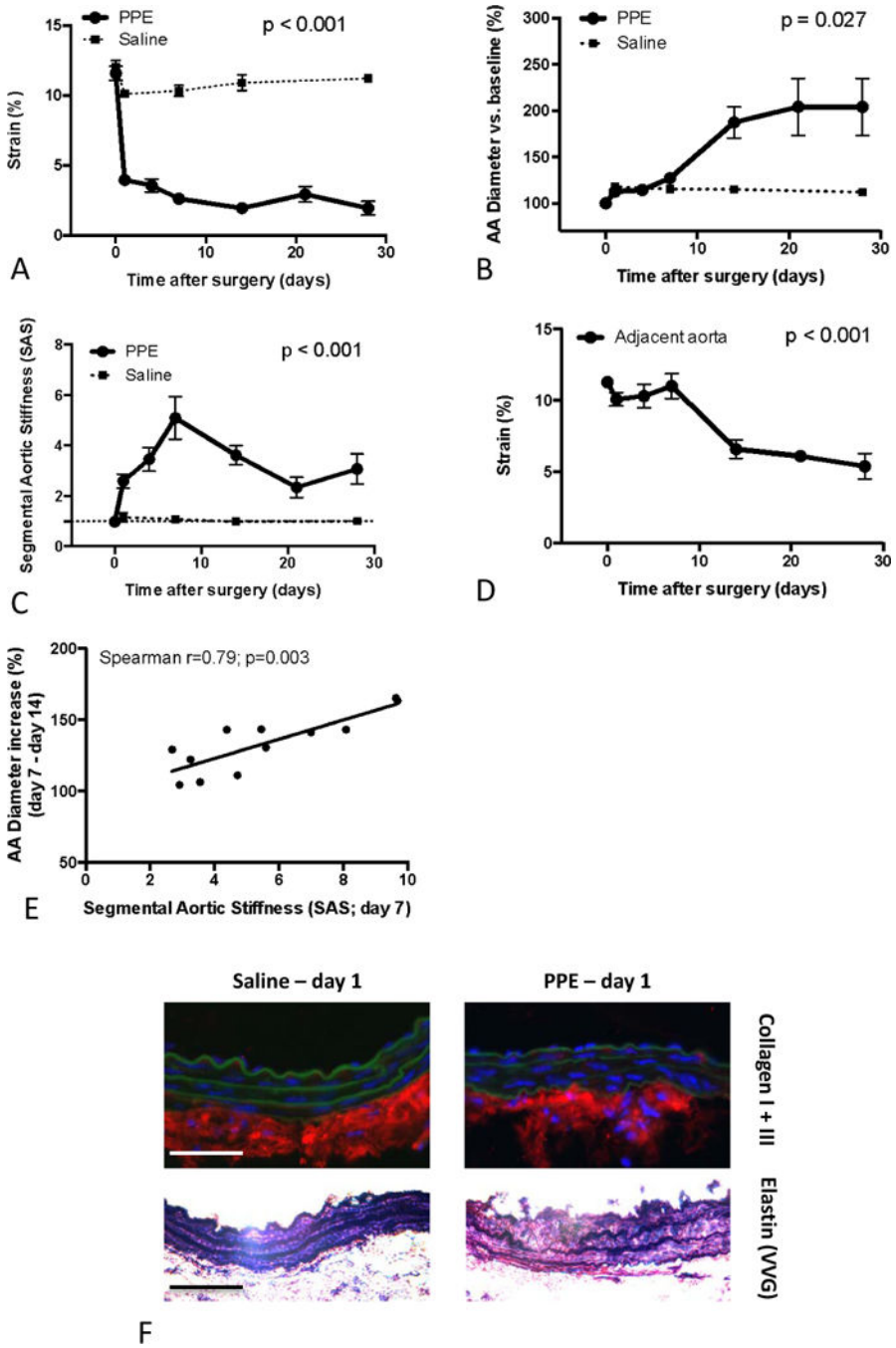

Figure 2.

Analysis of Segmental Aortic Stiffening and aneurysm progression in the PPE model. **(A)** Temporal development of circumferential cyclic strain of PPE- and saline-treated segments. **(B)** Diameter development of the PPE- and saline-treated segments (% vs. baseline (d0)). **(C)** Temporal analysis of Segmental Aortic Stiffness (SAS) of the PPE- or saline-treated segment relative to the adjacent abdominal aorta. **(D)** Temporal analysis of the circumferential cyclic strain of the adjacent aorta (bold line) in relation to the PPE-treated segment (thin line). **(E)** Correlation between the Segmental Aortic Stiffness (SAS) at d7 and

the consecutive diameter increase of the PPE-treated segment in the following 7 days. **(F)** Upper panels: Representative immunofluoresence staining for collagen I + III (red) with green autofluorescence of elastin lamellae. Lower panels: Modified Elastin Verhoeff's Van Gieson (VVG) staining. Data are mean±SEM. n=5–13 for each condition/time point; p values denote differences between PPE and saline groups by permutation F-test (A–C), aortic strain differences in PPE treated animals over time by Friedman's test (D), or significance level of Spearman correlation (E).

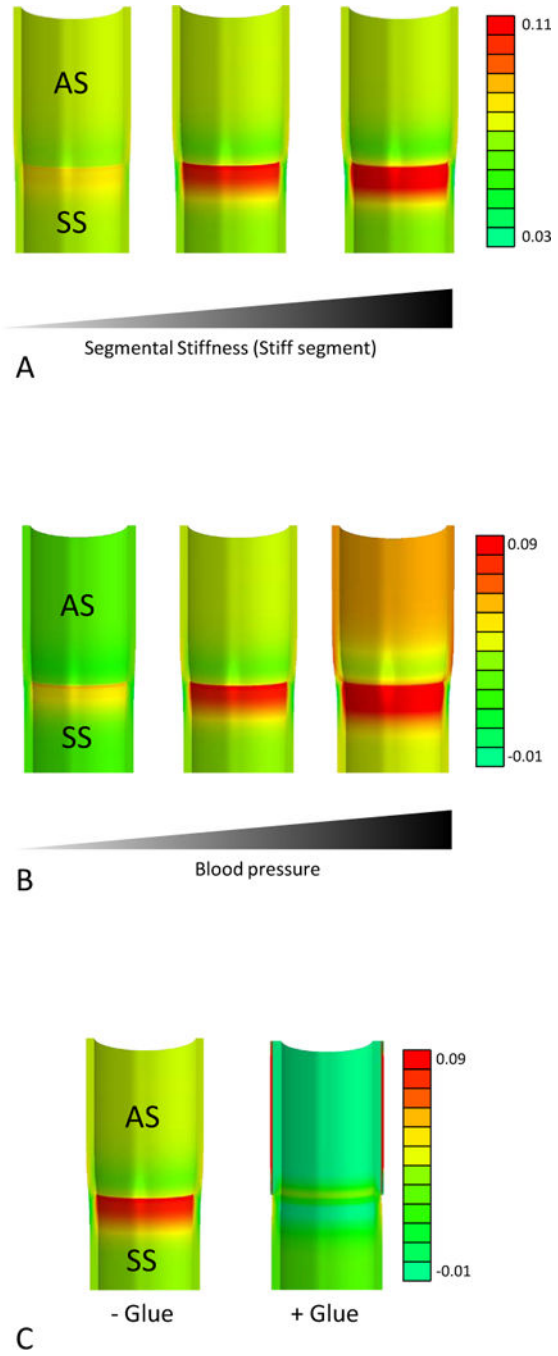

Figure 3.

Finite elements model (FEA) based axial stress analysis of segmental aortic stiffening. A simplified model of the murine infrarenal aorta was subjected to various mechanical conditions and resulting axial (longitudinal) stress (N/mm^2) was depicted. **(A)** The stiffness of the stiff aortic segment (SS) was increased (Shear moduli: 500 kPa left vessel, 1100 kPa middle vessel, 1700 kPa right vessel) to demonstrate the impact of segmental stiffness on axial stress generation. **(B)** The intraluminal pressure was increased (left vessel: 80 mmHg, middle vessel: 130 mmHg, right vessel: 180 mmHg) to visualize the influence of blood

pressure on axial stresses in a segmentally stiff aorta. **(C)** A segmentally stiff aorta (left) is subjected to external stiffening of the adjacent compliant segments (simulating glue treatment; right) to demonstrate axial stress reduction and homogenization induced by the intervention.

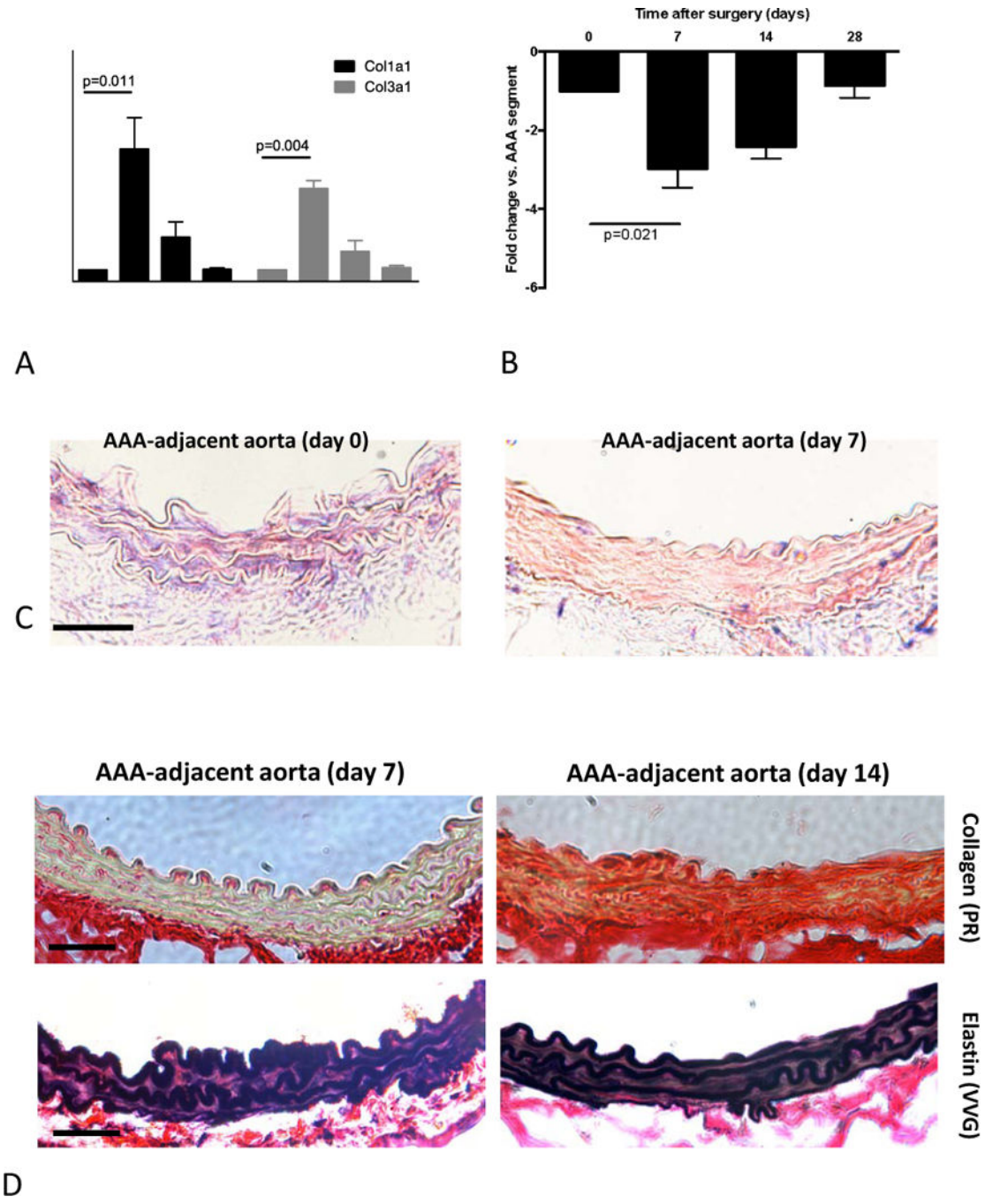

Figure 4.

Stiffening mechanisms of the AAA-adjacent aorta. **(A)** Temporal analysis of the *Col1a1* and *Col3a1* gene expression in the AAA-adjacent aorta compared to the AAA (PPE-treated) segment. **(B)** Temporal analysis of miR-29b expression in the AAA-adjacent aorta compared to the AAA (PPE-treated) segment. **(C)** *in situ* hybridization for miR-29b (purple-blue dye) and red nuclear counterstain in the AAA-adjacent aortic segments (original magnification 400×, scale bar 50 μm) **(D)** Representative images of the aortic wall taken from AAA-adjacent aortic segments 7 days or 14 days after PPE-treatment stained with

Picrosirius Red (upper panels; red: collagen; yellow: muscle) and Elastin VVG staining (lower panels). Original magnification 400×, scale bar 50 μm. * indicates $p<0.05$ vs. all other time points; # indicates $p<0.05$ vs. d0 and d28. n=5 for each time point; p values denote differences between expression levels by Kruskal-Wallis test with Dunn's post test.

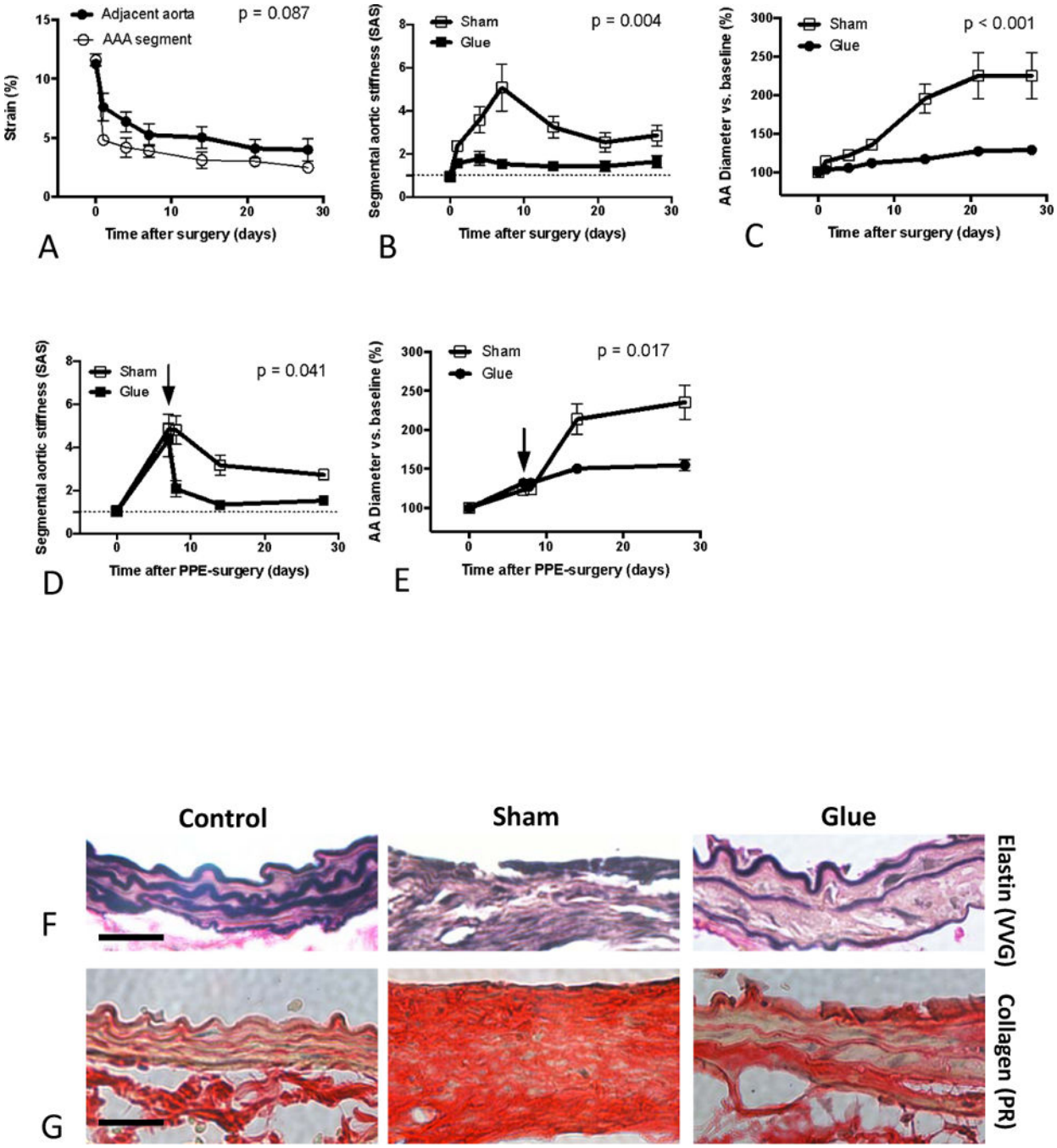

Figure 5.

Effects of glue-treatment on Segmental Aortic Stiffness and aneurysm progression. **(A)** Temporal analysis of the circumferential cyclic strain of the glue-treated adjacent aorta (bold line) in relation to the PPE-treated segment (thin line). **(B)** Temporal analysis of Segmental Aortic Stiffness (SAS) in glue-treated aortas compared to sham-glue-treated conditions. **(C)** Diameter development of the PPE-treated segment in glue-treated vs. sham-glue-treated conditions. Temporal development of SAS **(D)** and aortic diameter **(E)** following delayed glue or sham treatment 7 days after PPE surgery (arrows). Representative Elastin VVG

staining **(F)** or Picrosirius Red staining **(G)** of the aortic wall taken from native abdominal aortas (control) or PPE-treated segments (d14) after additional treatment of the adjacent aorta with glue or sham-glue (original magnification 400×; scale bars 50 μm). EVG staining was used to depict the integrity of the medial elastin lamellae. Picrosirius Red staining aided the visualization of the aortic wall architecture and collagen remodeling. n=7 for each time point; p values denote differences between aortic segments (A) or treatment groups (B–E) by permutation F-test.

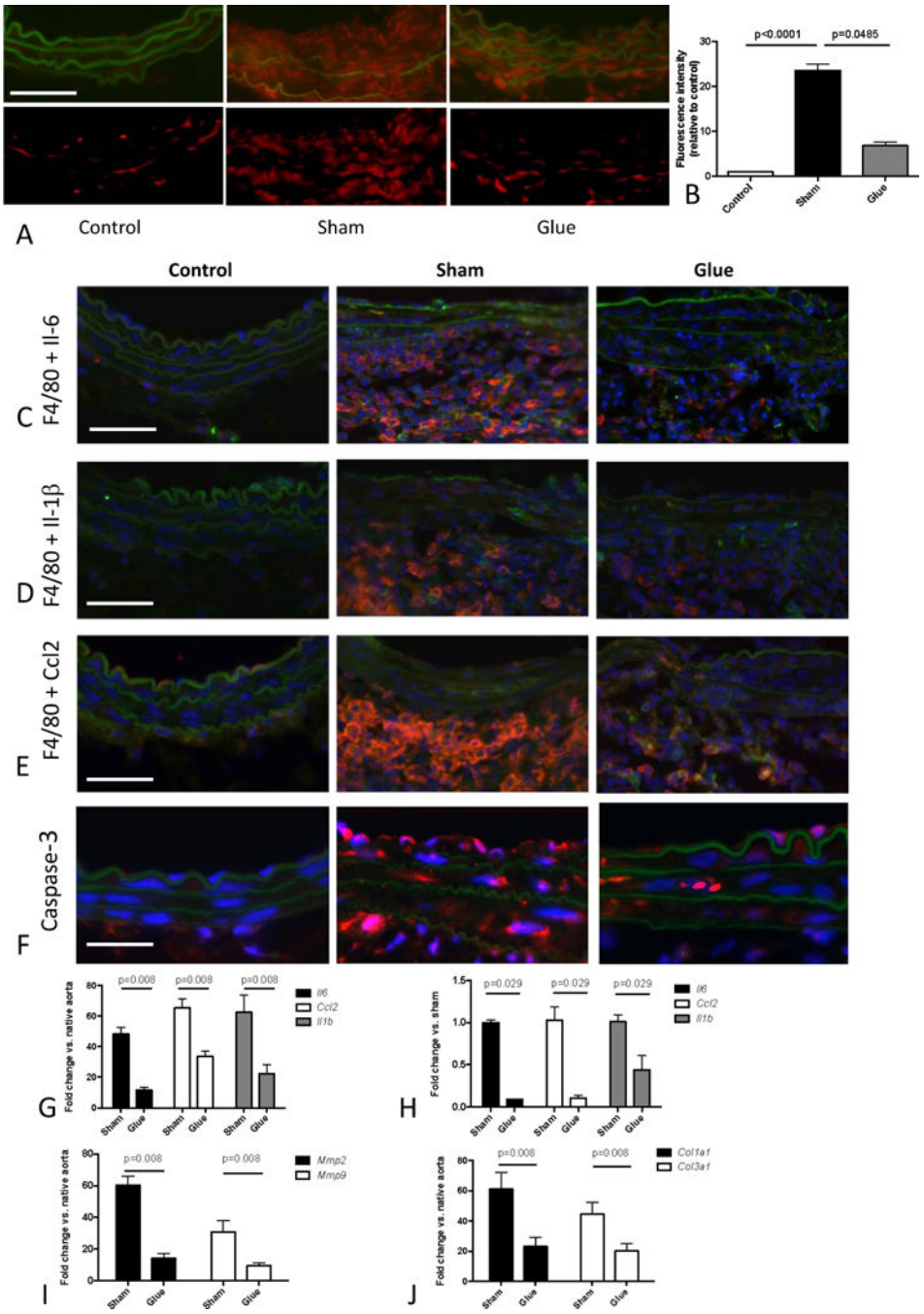

Figure 6.

Effects of glue-induced aortic stiffening on ROS generation and parameters of inflammation, apoptosis and ECM remodeling. **(A)** In situ DHE staining of native abdominal aortas (control) or PPE-treated segments after additional treatment of the adjacent aorta with glue or sham-glue (d7). ROS production was indicated by red fluorescence. Autofluorescence from elastic lamellae (depicted in green in the upper row) was subtracted (bottom row). Original magnification x400, scale bar 50 μm. **(B)** Average fluorescence was quantified from 3 high power fields of 3 different aortas per group. **(C,D,E)** Representative

co-staining of macrophages (red F4/80 marker) and the green labeled cytokines IL-6 (C), Il-1β (D) and Ccl2 (E) in native abdominal aortas (control) or PPE-infused segments (d7) after additional treatment of the adjacent aorta with glue or sham-glue (original magnification 400×, scale bar 50μm). Colocalization results in orange/yellow color. Nuclei are Hoechst stained (blue). **(F)** Corresponding immunostaining of activated caspase-3 (red). **(G, H)** Expression of *Il6, Ccl2,* and *Il1b* in the PPE-infused segment (d7) after additional glue or sham-glue treatment of the adjacent aorta, quantified in whole tissue (G) as well as in laser-captured macrophages.(H). Expression analysis of *Mmp2* and *Mmp9* **(I)** as well as *Col1a1* and *Col3a1* **(J)** (all vs. native control) in the PPE-infused segment (d7) after additional glue or sham-glue treatment of the adjacent aorta; p values denote differences between treatment groups by Kruskal-Wallis test with Dunn's post test (B) or Mann-Whitney test (G–J).

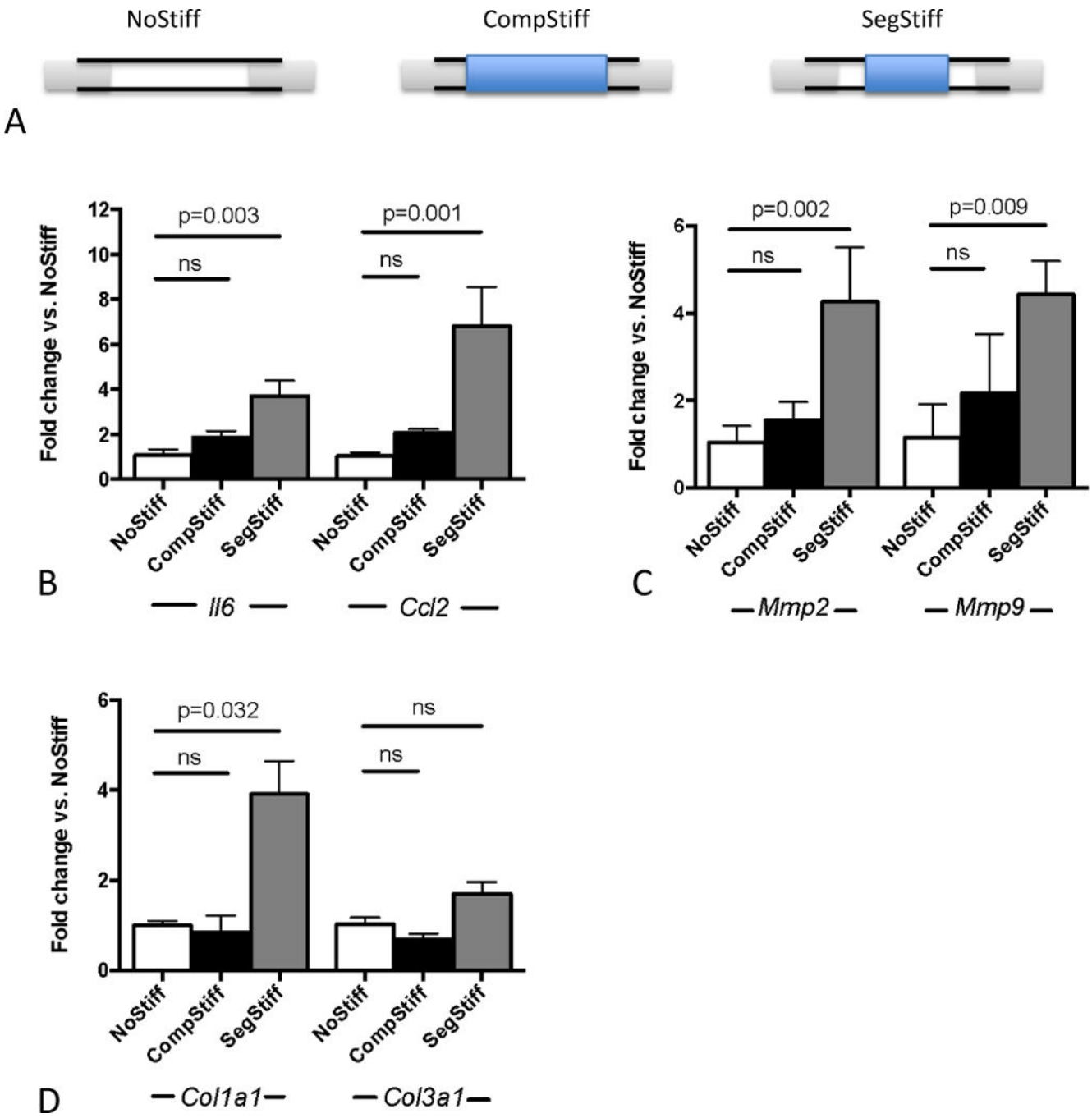

Figure 7.

Ex vivo aortic mechanical stimulation. **(A)** Scheme of the experimental setup for differential mechanical stimulation of the cannulated aorta. Cyclic strain is imposed on unrestrained/ unstiffened aortas (NoStiff), completely restrained aorta (CompStiff) or segmentally restrained aorta (SegStiff). **(B–D)** Gene expression results after one hour of mechanical stimulation in the 3 groups. Depicted is the differential expression of inflammation related genes *Il6* and *Ccl2* (B), matrix metalloproteinases *Mmp2* and *Mmp9* (C) and collagen genes

Col1a1 and *Col3a1* (D) (all vs. NoStiff condition). n=5 for each condition; p values denote differences between treatment groups by Kruskal-Wallis test with Dunn's post test.

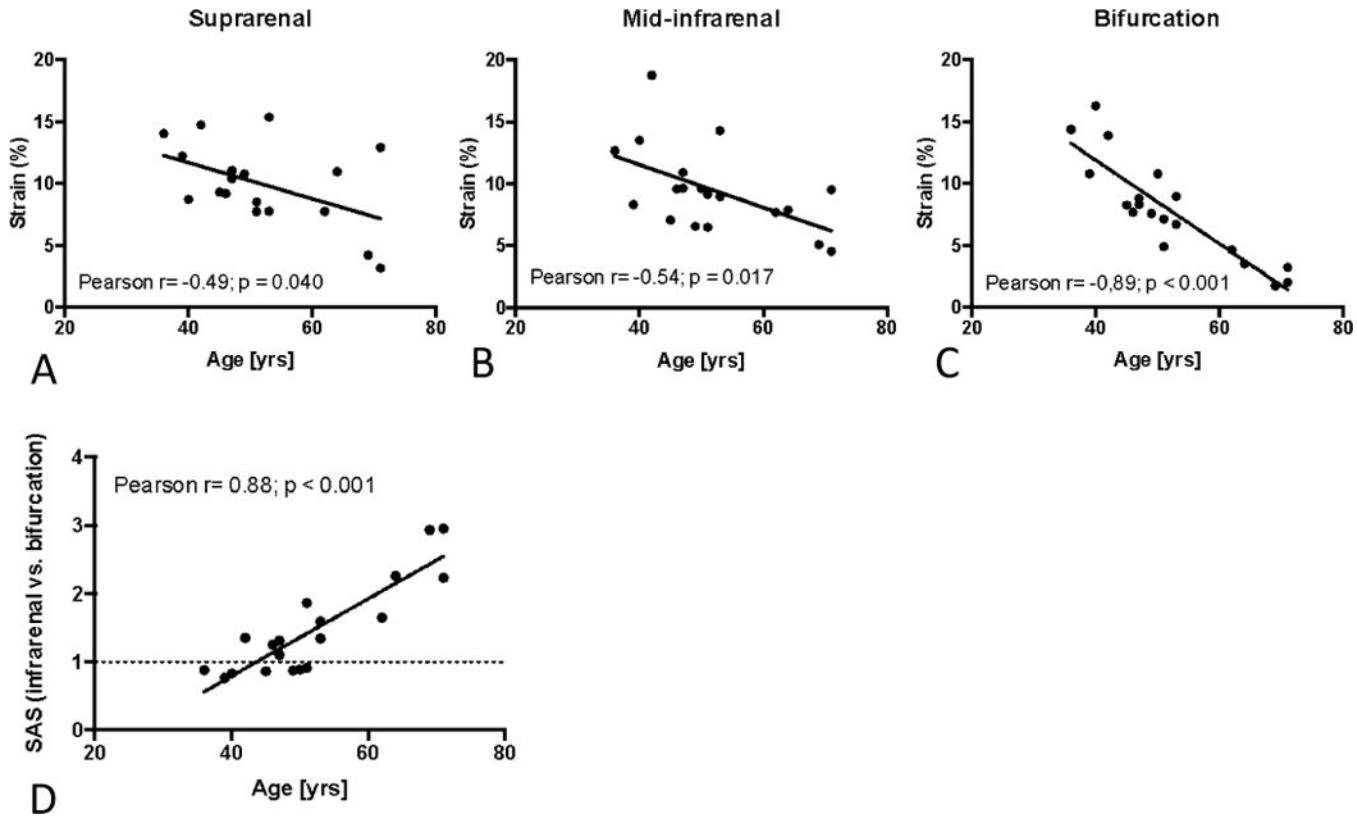

Figure 8.

Segmental Aortic Stiffening in the aging human abdominal aorta. **(A–C)** Correlation between age and circumferential cyclic strain in the supra-renal (A), mid-infrarenal (B) and bifurcational segment (C) of the human abdominal aorta. **(D)** Correlation between age and segmental stiffness (SAS, bifurcational segment vs. mid-infrarenal segment) along the infrarenal abdominal aorta; p denotes significance level of Pearson correlation.